Proceedings of International Conference on Heat Exchanger Fouling and Cleaning - 2015 (Peer-reviewed)
June 07 - 12, 2015, Enfield (Dublin), Ireland
Editors: M.R. Malayeri, H. Müller-Steinhagen and A.P. Watkinson
Published online
www.heatexchanger-fouling.com

STREAM FLOW RATE OPTIMIZATION FOR FOULING MITIGATION IN THE PRESENCE OF THERMOHYDRAULIC CHANNELING

R. L. da Silva[1], A. L. H. Costa[1], and E. M. Queiroz[3]

[1] Rio de Janeiro State University (UERJ), Rua São Francisco Xavier, 524, Rio de Janeiro, RJ, Brazil - andrehc@uerj.br
[2] Federal University of Rio de Janeiro (UFRJ), Centro de Tecnologia, Cidade Universitária, Rio de Janeiro, RJ, Brazil

ABSTRACT

The accumulation of deposits decreases the thermal effectiveness of heat exchangers. However, fouling effects are not limited to the thermal behaviour; it also affects the hydraulic behaviour of heat exchangers, causing an increase in the flow resistance. Despite its importance, this interrelation between thermal and hydraulic behaviors is often ignored. In systems composed of parallel units, this phenomenon can modify the flow distribution among individual heat exchangers, i.e. dirtier units are associated to larger flow resistances, which tend to diminish the flow rate in those units. In fact, the problem is recursive, because smaller flow rates are also associated with lower velocities, which determine larger fouling rates. This flow disturbance associated with the fouling pattern between parallel units is called thermo-hydraulic channeling. This paper presents the optimization of the flow rate distribution in parallel units in order to mitigate fouling. The objective function involves the minimization of the energy consumption and production losses. The constraints are composed of mass, energy and mechanical energy balances, fouling rate modelling and heat transfer equations. The solution indicates the profiles of the flow rate distribution, which minimizes the fouling impact during a certain operational horizon. The performance of the proposed approach is illustrated through its application to a system composed of two heat exchangers in parallel.

INTRODUCTION

Fouling in heat exchangers corresponds to the undesirable accumulation of deposits over the heat transfer surface. This phenomenon introduces an extra resistance in the thermal circuit, which causes a decrease in the heat exchanger thermal effectiveness due to the reduction in the overall heat transfer coefficient. Fouling brings several economic impacts such as increase of utility consumption associated with the reduction in the heat exchanged among process streams, additional maintenance costs associated with cleaning activities, larger capital costs because of the necessary increase in the heat exchangers area, and production losses when the fouling is so severe that is necessary to decrease the plant throughput.

An important aspect of the fouling problem, that is usually ignored, corresponds to its hydraulic impact. The deposit layer that is formed increases the flow resistance along the thermal equipment. This effect can be caused by the reduction in the flow area, increase in the surface roughness or even the interruption of the flow along certain paths (e.g. tubes entirely blocked by deposits) (Yeap et al., 2005). In regular conditions, the opening of the control valves compensates the increase in the flow resistance. However, if there is an intense deposit accumulation in a hydraulic constrained system, the control valves can be saturated. In this case, there is a reduction in the flow rate. In heat exchanger networks, the hydraulic impact of fouling can be quite complex, because the different fouling levels in the heat exchangers can modify the flow rate distribution along the equipment.

In fact, the thermal and hydraulic effects of fouling can present a direct interrelation. In thermal systems composed of parallel equipment, the dirtier units may present lower flow rates due to the larger flow resistances caused by fouling. Due to the flow reduction, it will occur a diminution of the flow velocity and the fouling rate in these units will increase. As a consequence, there is a feedback effect, where the uneven fouling determines a flow rate distribution disturbance, which intensifies the fouling itself in the dirtier heat exchangers. This phenomenon was called thermo-hydraulic channeling by Ishiyama et al. (2008). Aiming to mitigate this problem, the authors suggested the installation of control valves able to guarantee equal flow rates along the parallel equipment. According to a simulation example, this policy reduced the energy consumption and the production losses.

In this context, this paper investigates the optimization of the flow rate distribution among parallel units for fouling mitigation. This approach was also investigated by Oliveira Filho et al. (2009), Assis et al. (2013), and Assis et al. (2015), but the association of thermal and hydraulic effects was not handled in any of these references.

The target of the proposed optimization scheme is to reduce the energy and production loss penalties caused by fouling. The heat exchanger network model employed is composed of mass, energy and mechanical energy balances, fouling rate equations, and heat transfer equations. The optimization structure corresponds to a mathematical programming problem organized as a nonlinear programming problem (NLP).

PROBLEM FORMULATION

The optimization seeks to identify the flow rates associated to the minimum penalty cost caused by fouling during a certain time horizon. This set of flow rates must be related to the existent control valves in the hydraulic network, according to mechanical energy balances.

The problem is addressed considering that fouling only occurs in the cold streams that flow through the tube-side, according to the Ebert-Panchal model. However, the formulation is general and could be adapted for other situations, depending on the availability of the corresponding fouling rate model.

Network structure

The network structure is represented as a digraph. The vertices, identified by the index $t \in VET$, represent the network equipment and are organized in the following subsets: *HE* for heat exchangers, *MX* for mixers, *SP* for splitters, *PU* for pumps, and *PS* and *PD* for supply and demand units. The edges represent the streams, identified by the index $k \in STR$, partitioned into the subsets *HSTR* for hot streams and *CSTR* for cold streams. In the hydraulic analysis, the network is partitioned into sections, $s \in S$, where each section is composed by a set of parallel branches, $r \in R_s$. Due to the dynamic nature of the problem, all variables are also identified by a time index $\tau \in TI$.

Optimization variables

The variables $m_{k,\tau}$ and $T_{k,\tau}$ identify the mas flow rate and temperature of process streams. The variables $n_{t,\tau}$ and $V_{t,\tau}$ identify the network inlet/outlet mass flow rate and temperature through a supply/demand vertex. Heat load, dirty overall heat transfer coefficient, film transfer coefficients and the dimensionless groups of the P-NTU method of a heat exchanger are represented, respectively, by $Q_{t,\tau}$, $U_{t,\tau}$, $h_{tube,t,\tau}$, $h_{shell,t,\tau}$, $CR_{t,\tau}$, $NTU_{t,\tau}$, and $P_{t,\tau}$.

The fouling model variables encompass the fouling resistance, $R_{f,t,\tau}$, the average fouling rate and the fouling rate at the exchanger ends, $dRfdt_{t,\tau}$, $dRfdt_{1,t,\tau}$, $dRfdt_{2,t,\tau}$, and the film and surface temperatures at the exchanger ends, $T_{film1,t,\tau}$, $T_{film2,t,\tau}$, $T_{s1,t,\tau}$, $T_{s2,t}$.

The variables of the hydraulic model are the fouled inner pipe diameter, $D_{i,f,t,\tau}$, the thickness of the deposit layer $\delta_{f,t,\tau}$, the pipe and fouled heat exchanger tubes velocities, $v_{pipe,k,\tau}$ and $v_{f,t,\tau}$, the Reynolds number in the pipe flow and in the fouled heat exchanger tube-side, $Re_{pipe,k,\tau}$ and $Re_{f,t,\tau}$, the Fanning friction factor in the pipes and in the heat exchanger tube-side, $f_{pipe,k,\tau}$ and $f_{f,t,\tau}$, and the valve lift position, $x_{k,\tau}$.

The pressure drops in the fouled heat exchangers, valves, pipes and the pump pressure increase are represented by $\Delta P_{f,t,\tau}$, $\Delta P_{valve,k,\tau}$, $\Delta P_{pipe,k,\tau}$, and $\Delta P_{pump,t,\tau}$. The pressure drops along the branches are represented by $\Delta P_{BR,r,\tau}$ and the pressure drops in the network sections are given by $\Delta P_{SE,s,\tau}$.

Objective function

The main goal of the optimization is to minimize two economic penalties caused by fouling during the system operation: the increase of the utility consumption due to the reduction of the total network heat load and the production losses due to the hydraulic limitations. Considering that the fouling penalties varies dynamically, these terms are described in the objective function by two summations related to a numerical integration procedure:

$$fobj = \sum_{t\in PD}\sum_{\tau\in TI} p_\tau s_\tau C_{OP,t} n_t CP_t (V_{ref,t} - V_{t,\tau}) + \sum_{t\in PD}\sum_{\tau\in TI} p_\tau s_\tau C_{lo}(n_{t,\tau}^{spt} - n_{t,\tau}) \quad (1)$$

where p_τ are the weights of the numerical integration procedure (e.g. Simpson rule), s_τ are the present worth factors, $C_{OP,t}$ is the utility cost associated to the outlet stream of vertex *t*, C_{lo} is the production loss unitary cost, *ref* is a subscript associated to the temperature specification for energy consumption evaluation, and *spt* is a superscript associated to the flow rate set-point.

Constraints

Mass balances. The mass balances at the network vertices are given by:

$$\sum_{k\in S_t^{in}} m_{k,\tau} - \sum_{k\in S_t^{out}} m_{k,\tau} = 0 \quad t\in(MX\cup SP\cup PU), \tau\in TI \quad (2)$$

$$\sum_{k\in S_t^{in}} m_{k,\tau} - \sum_{k\in S_t^{out}} m_{k,\tau} + n_t = 0 \quad t\in(PS\cup PD), \tau\in TI \quad (3)$$

$$\sum_{k\in(S_t^{in}\cap HSTR)} m_{k,\tau} - \sum_{k\in(S_t^{out}\cap HSTR)} m_{k,\tau} = 0 \quad t\in HE, \tau\in TI \quad (4)$$

$$\sum_{k\in(S_t^{in}\cap CSTR)} m_{k,\tau} - \sum_{k\in(S_t^{out}\cap CSTR)} m_{k,\tau} = 0 \quad t\in HE, \tau\in TI \quad (5)$$

where the superscripts *in* and *out* identify the set of edges S_t that is direct to/from the vertex *t*

Energy balances. The energy balances at the network vertices are given by:

$$\sum_{k\in S_t^{in}} m_{k,\tau} Cp_k T_{k,\tau} - \sum_{k\in S_t^{out}} m_{k,\tau} Cp_k T_{k,\tau} = 0 \quad t\in(MX\cup SP\cup PU), \tau\in TI \quad (6)$$

$$\sum_{k\in S_t^{in}} m_{k,\tau} Cp_k T_{k,\tau} - \sum_{k\in S_t^{out}} m_{k,\tau} Cp_k T_{k,\tau} + n_t CP_t V_{t,\tau} = 0 \quad t\in(PS\cup PD), \tau\in TI \quad (7)$$

$$\sum_{k\in(S_t^{in}\cap HSTR)} m_{k,\tau} Cp_k T_{k,\tau} - \sum_{k\in(S_t^{out}\cap HSTR)} m_{k,\tau} Cp_k T_{k,\tau} - Q_{t,\tau} = 0 \quad t\in HE, \tau\in TI \quad (8)$$

$$\sum_{k\in(S_t^{in}\cap CSTR)} m_{k,\tau} Cp_k T_{k,\tau} - \sum_{k\in(S_t^{out}\cap CSTR)} m_{k,\tau} Cp_k T_{k,\tau} + Q_{t,\tau} = 0 \quad t\in HE,\tau\in TI \tag{9}$$

$$T_{k,\tau} - T_{k',\tau} = 0 \quad t\in SP, k\in S_t^{in}, k'\in S_t^{out}, \tau\in TI \tag{10}$$

$$V_{t,\tau} - V_{t,\tau}^{spe} = 0 \quad t\in PS,\tau\in TI \tag{11}$$

where Cp_k is the heat capacity of the stream k, CP_t is the heat capacity of the inlet/outlet stream through the supply/demand vertex t, and the superscript *spe* identifies the specifications of the network inlet temperature at the supply units.

Heat exchangers equations. The heat transfer in the heat exchangers is described using the P-NTU method (Shah and Sekulic, 2003), based on the following equations, related to the effectiveness, number of heat transfer units and ratio between heat capacity flow rates:

$$P_{t,\tau}T_{k,\tau} + (1-P_{t,\tau})T_{k',\tau} - T_{k'',\tau} = 0 \quad t\in HE,\ k\in(CSTR\cap S_t^{in}),\ k'\in(HSTR\cap S_t^{in}),\ k''\in(HSTR\cap S_t^{out}),\tau\in TI \tag{12}$$

$$NTU_{t,\tau} m_{k,\tau} Cp_k - U_{t,\tau} A_t = 0 \quad t\in HE,\ k\in(HSTR\cap S_t^{in}),\tau\in TI \tag{13}$$

$$CR_t m_k Cp_k - m_{k'} Cp_{k'} = 0 \quad t\in HE,\ k\in(CSTR\cap S_t^{in}),\ k'\in(HSTR\cap S_t^{in}),\tau\in TI \tag{14}$$

Two heat exchangers configurations are considered: countercurrent flow or multipass configuration with an even number of passes in the tube-side. The corresponding P-NTU expressions are, respectively:

$$P_{t,\tau} - \frac{1-\exp[-NTU_{t,\tau}(1-CR_{t,\tau})]}{1-CR_{t,\tau}\exp[-NTU_{t,\tau}(1-CR_{t,\tau})]} = 0 \quad t\in SCC\subset HE,\tau\in TI \tag{15}$$

$$P_{t,\tau} - 2\left\{1+CR_{t,\tau}+(1+CR_{t,\tau}^2)^{0.5}Z_{t,\tau}\right\}^{-1} = 0$$
$$Z_{t,\tau} = \frac{1+\exp[-NTU_{t,\tau}(1+CR_{t,\tau}^2)^{0.5}]}{1-\exp[-NTU_{t,\tau}(1+CR_{t,\tau}^2)^{0.5}]} \quad t\in SMP\subset HE,\tau\in TI \tag{16}$$

where *SCC* and *SMP* are the subsets of heat exchangers with countercurrent or multipass configurations.

The overall heat transfer coefficient in the dirty condition is given by:

$$\frac{1}{U_{t,\tau}} - \frac{1}{h_{shell,t,\tau}}\left(\frac{D_{i,t}}{D_{e,t}}\right) - \frac{D_{i,t}\log(D_{e,t}/D_{i,t})}{2k_{w,t}} - \frac{1}{h_{tube,t,\tau}} - R_{f,t,\tau} = 0 \quad t\in HE,\tau\in TI \tag{17}$$

where $D_{i,t}$ and $D_{e,t}$ are the inner and outer tube diameters, and $k_{w,t}$ is the thermal conductivity of the tube wall. In Eq. (17), it is assumed that the fouling is limited to the tube-side, coherent with the fouling rate model discussed in the next sub-section.

The evaluation of the tube-side and shell-side heat transfer coefficients can be given by:

$$h_{tube,t} - h_{tube,t}^{base}\left(\frac{m_k}{m_{tube,t}^{base}}\right)^{0.8} = 0 \quad t\in HE,\ k\in(CSTR\cap S_t^{in}),\tau\in TI \tag{18}$$

$$h_{shell,t} - h_{shell,t}^{base}\left(\frac{m_k}{m_{shell,t}^{base}}\right)^{0.6} = 0 \quad t\in HE,\ k\in(HSTR\cap S_t^{in}),\tau\in TI \tag{19}$$

where the superscript *base* indicates a base case related to the heat exchanger design. According to these equations, the cold streams flow in the tube-side.

Fouling rate model. In this analysis, the fouling rate can be described by the modified Ebert-Panchal model (Ishiyama et al., 2008).

The constraints related to the fouling rate model are given by:

$$dRfdt_{t,\tau} = 0.5(dRfdt_{1,t,\tau} + dRfdt_{2,t,\tau}) \quad t\in HE,\tau\in TI \tag{20}$$

$$dRfdt_{1,t,\tau} \geq \alpha\,\mathrm{Re}_{f,t,\tau}^{-0.66}\mathrm{Pr}_t^{0.33}\exp(-E_a R_{gas}^{-1} T_{film1,t,\tau}^{-1})) - -\gamma(f_{f,t,\tau}\rho_t v_{t,\tau}^2/2) \quad t\in HE,\tau\in TI \tag{21}$$

$$dRfdt_{2,t,\tau} \geq \alpha\,\mathrm{Re}_{f,t,\tau}^{-0.66}\mathrm{Pr}_t^{0.33}\exp(-E_a R_{gas}^{-1} T_{film2,t,\tau}^{-1})) - -\gamma(f_{f,t,\tau}\rho_t v_{t,\tau}^2/2) \quad t\in HE,\tau\in TI \tag{22}$$

$$\mathrm{Re}_{f,t,\tau} - D_{i,f,t,\tau} v_{f,t,\tau}\rho_t/\mu_t = 0 \quad t\in HE,\tau\in TI \tag{23}$$

$$dRfdt_{1,t,\tau} \geq 0 \quad t\in HE,\tau\in TI \tag{24}$$

$$dRfdt_{2,t,\tau} \geq 0 \qquad t \in HE, \tau \in TI \qquad (25)$$

where α, Ea and γ are fouling rate parameters, and R_{gas} is the universal gas constant.

These constraints are complemented by the following set of mathematical relations for the evaluation of Fanning friction factor, fluid flow velocity, and film and surface temperatures:

$$f_{f,t,\tau} = 0.0035 + 0.264(\mathrm{Re}_{f,t,\tau})^{-0.42} \quad t \in HE, \tau \in TI \qquad (27)$$

$$v_{f,t,\tau} - \frac{4m_{t,\tau}N_{pt,t}}{\rho_t \pi (D_{i,f,t,\tau})^2 N_{tt,t}} = 0 \qquad t \in HE,\ k \in (CSTR \cap S_t^{in}), \tau \in TI \qquad (28)$$

$$T_{film1,t,\tau} = 0.5(T_{s1,t,\tau} + T_{k,\tau}) \qquad t \in HE,\ k \in (CSTR \cap S_t^{in}), \tau \in TI \qquad (29)$$

$$T_{film2,t,\tau} = 0.5(T_{s2,t,\tau} + T_{k,\tau}) \qquad t \in HE,\ k \in (CSTR \cap S_t^{out}), \tau \in TI \qquad (30)$$

$$\frac{T_{s1,t,\tau} - T_{k,\tau}}{\frac{1}{h_{tube,t,\tau}}} = \frac{T_{k',\tau} - T_{s1,t,\tau}}{\frac{1}{h_{shell,t,\tau}D_{e,t}} + \frac{\log(D_e/D_i)}{2k_w} + \frac{R_{f,t,\tau}}{D_{i,t}}}$$
$$t \in HE,\ k \in (CSTR \cap S_t^{in}), k' \in (HSTR \cap S_t^{out}), \tau \in TI \qquad (31)$$

$$\frac{T_{s2,t,\tau} - T_{k,\tau}}{\frac{1}{h_{tube,t,\tau}}} = \frac{T_{k',\tau} - T_{s2,t,\tau}}{\frac{1}{h_{shell,t,\tau}D_{e,t}} + \frac{\log(D_e/D_i)}{2k_w} + \frac{R_{f,t,\tau}}{D_{i,t}}}$$
$$t \in HE,\ k \in (CSTR \cap S_t^{out}), k' \in (HSTR \cap S_t^{in}), \tau \in TI \qquad (32)$$

where N_{pt} is the number of tube passes, N_{tt} is the total number of tubes, and k_w is the thermal conductivity of the tube wall.

Hydraulic model. The hydraulic model is limited to the flow of the cold stream. The pressure drops in the heat exchangers, pipes, valves, and the pump head are given by:

$$\Delta P_{HE,t,\tau} - \frac{4f_{f,t,\tau}\rho_t N_{pt,t} L_t v_{f,t,\tau}^2}{2D_{i,f,t,\tau}} - K_t \rho_t N_{pt,t} \frac{v_{f,t,\tau}^2}{2} = 0 \qquad t \in HE, \tau \in TI \qquad (33)$$

$$\Delta P_{pipe,k,\tau} - \frac{4f_{pipe,t,\tau}\rho_{pipe,k} L_{pipe} v_{pipe,k,\tau}^2}{2d_{pipe,k}} = 0 \qquad k \in CSTR, \tau \in TI \qquad (34)$$

$$\Delta P_{valve,k,\tau} - \rho_{pipe,k} \frac{\left(m_k/\rho_{pipe,k}\right)^2}{R_k^{x_{k,\tau}-1} Cv_k} = 0 \qquad k \in valve, \tau \in TI \qquad (35)$$

$$\Delta P_{pump,t,\tau} - (-a_t m_k^2/\rho_{pipe,k}^2 + b_t m_k/\rho_{pipe} + c_t)\rho_{pipe,k} g = 0 \qquad t \in PU,\ k \in (CSTR \cap S_t^{in}), \tau \in TI \qquad (36)$$

where a_t, b_t and c_t are the coefficients of the polynomial which describes the pump curve, R_k and Cv_k are valve coefficients.

The flow velocities, Reynolds number and Fanning friction factor in the pipes are evaluated by:

$$v_{pipe,k,\tau} - \frac{4m_{k,\tau}}{\rho_{pipe,k}\pi (d_{k,\tau})^2} = 0 \quad k \in CSTR, \tau \in TI \qquad (37)$$

$$\mathrm{Re}_{pipe,k,\tau} - d_k v_{pipe,k,\tau} \rho_{pipe,k}/\mu_{pipe,k} = 0 \qquad k \in CSTR, \tau \in TI \qquad (38)$$

$$f_{pipe,k,\tau} = 0.0035 + 0.264(\mathrm{Re}_{pipe,k,\tau})^{-0.42} \qquad k \in CSTR, \tau \in TI \qquad (39)$$

where d_k is the inner pipe diameter.

The layer of the deposits inside the heat exchanger tubes can be evaluated relating the fouling resistance to a conductive resistance expression, thus yielding:

$$\delta_{f,t,\tau} - \frac{D_{i,t,\tau}}{2} + \frac{D_{i,t,\tau}}{2\exp(\frac{2k_{f,t}R_{f,t,\tau}}{D_{i,t,\tau}})} = 0 \qquad t \in HE, \tau \in TI \qquad (40)$$

where $k_{f,t}$ is the thermal conductivity of the deposit.

The fouling inner diameter is given by:

$$D_{i,f,t.\tau} - (D_{i,t,\tau} - 2\delta_{f,t,\tau}) = 0 \quad t \in HE, \tau \in TI \qquad (41)$$

The pressure drop in each network branch is given by the sum of the pressure drops of the existent equipment:

$$\Delta P_{BR,r,\tau} - \sum_{k \in STR_r} \Delta P_{pipe,k,\tau} - \sum_{t \in (HE \cap VET_r)} \Delta P_{HE,t,\tau} - \sum_{k \in (valve \cap STR_r)} \Delta P_{valve,k,\tau} = 0 \qquad r \in R_s, \tau \in TI \qquad (42)$$

The pressure drop in a section is equal to the pressure drops of their parallel branches:

$$\Delta P_{SEC,s,\tau} - \Delta P_{BR,r,\tau} = 0 \qquad s \in S, r \in R_s, \tau \in TI \qquad (43)$$

The pressure drop along the sections must be equivalent to the pressure increase related to the pumps (difference of elevations and initial and final pressures are dismissed):

$$\sum_{s \in S} \Delta P_{SEC,s,\tau} - \sum_{s \in S} \sum_{t \in PU_s} \Delta P_{pump,t,\tau} = 0 \qquad \tau \in TI \qquad (44)$$

NUMERICAL RESULTS AND DISCUSSION

The application of the proposed procedure is illustrated using a small heat exchanger network composed of two identical shell-and-tube heat exchangers in parallel. The corresponding flowsheet is shown in Fig.1.

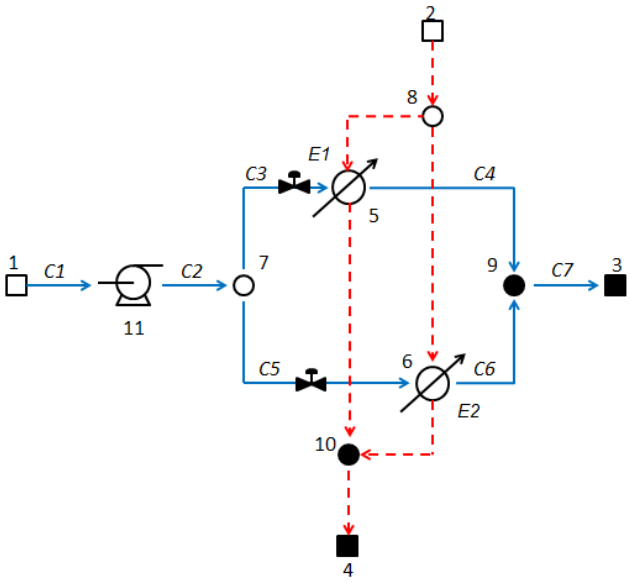

Fig.1 Heat exchanger network example

The data of the process streams are shown in Table 1.

Table 1. Stream data.

Variable	Cold stream	Hot stream
m (kg/s)	310	176
Inlet T (ºC)	157	214
Cp (J/kgK)	2378	2476
μ (Pa·s)	0.00124	-
ρ (kg/m^3)	818.8	-
k (W/m·K)	0.102	-

Each heat exchanger is composed of 1520 tubes of carbon steel (thermal conductivity equal to 55 W/m·K). The tubes are 6.1 m long with outer and inner diameter equal to 19.05 mm and 14.85 mm. The resultant heat transfer area is 555 m^2. The heat exchangers have two tube-side passes and one shell-side pass. The heat transfer coefficients at the base case are equal to 1365 W/m^{2}K for the tube-side and 1540 W/m^{2}K for the shell-side.

At the start of operation, one of the heat exchangers is dirty (E1) with a fouling resistance of $1 \cdot 10^{-5}$ m^{2}K/W, and the other is clean (E2) with a null fouling resistance. The values of fouling rate model parameters are: α = 127.7 m^{2}K/J, E_a = 76 kJ/mol and γ = $3.44 \cdot 10^{-15}$ m^2·K/(J·Pa). The thermal conductivity of the deposit is 0.7 W/m·K. The coefficients a, b and c of the pump curve are equal to, respectively: -35, 2 and 56.

The energy cost is 0.01 US$/MJ and the cost of the production loss is 0.05 US$/kg. The reference temperature for evaluation of the energy cost associated with the cold stream is 179.4 ºC, which corresponds to the network outlet temperature at the clean condition. The utility costs for hot stream cooling are not considered. The optimization is conducted in a five years horizon (280 weeks), using a time step of four weeks.

This example was implemented in the software GAMS 23.7, and the solver CONOPT was used for solving the optimization problem.

Aiming to evaluate the gain of the optimization procedure, the optimal results are compared with a base case where the heat exchanger flow rates are equal. Table 2 contains the corresponding values of the objective function.

Table 2. Objective function values.

	Optimal Case	Base case
Value (MM$)	504.52	594.24

The analysis of the objective function values indicate that the optimization allowed a total cost reduction of 15%.

The total flow rate of the cold stream in the optimization and in the base case are shown in Fig. 2.

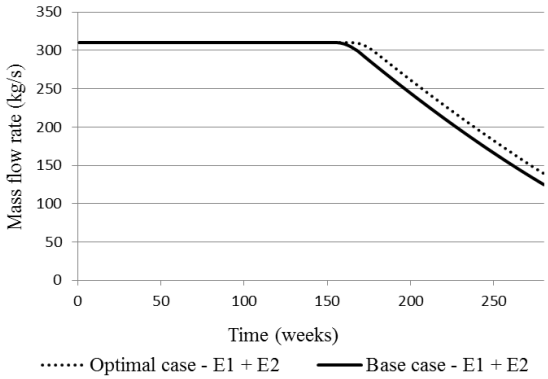

Fig. 2 Total mass flow rate of the cold stream for the optimal and base cases.

The profiles in Fig. 2 indicate that, in both cases, the deposit accumulation brings a reduction of the throughput due to the increase of the pressure drop in the heat exchangers. During an initial period, the increase of the heat exchangers pressure drop was compensated by the control valve opening, but later, after valve saturation (fully open), there is a flow rate reduction. However, after comparing both profiles, it is possible to observe that the optimization

identified an operational policy with larger flow rates, which mitigates production losses.

In the base case, the flow rates in the heat exchangers are kept equivalent, but in the optimization, their values are optimized according to control valve manipulation. The cold and hot stream flow rates in each heat exchanger are shown in Fig. 3 and Fig. 4. In the optimization, the cold stream is split almost equally during the initial period of the time horizon. Later, a larger fraction of the cold stream is directed to the initially clean heat exchanger. For the hot stream, there is an opposite distribution, where a larger fraction of the hot stream is directed to the initially dirty heat exchanger during almost the entire time horizon, and near the end of the period, the values tends to converge to a common level. Fig. 3 also contains the profile of the base case distribution, where both flow rates are equal.

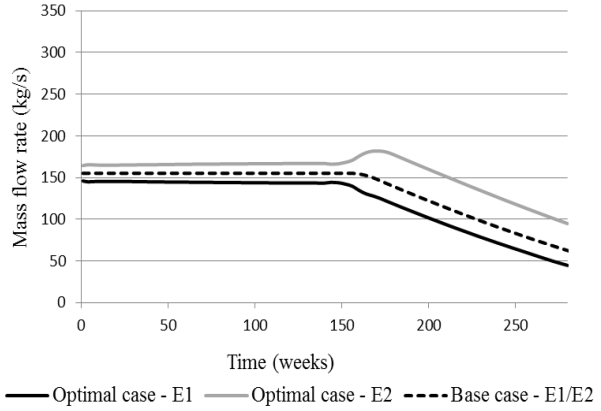

Fig. 3 Mass flow rates of the cold stream in the optimization.

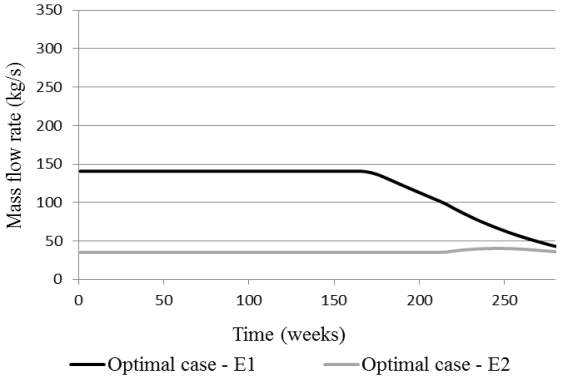

Fig. 4 Mass flow rates of the hot stream in the optimization.

The total heat duty in the heat exchangers indicates a continuous reduction due to fouling in Fig. 5. The comparison between the optimal case and the base case indicates that the base case presents a higher heat recovery during almost the entire horizon, but this gain do not financially compensate the production losses.

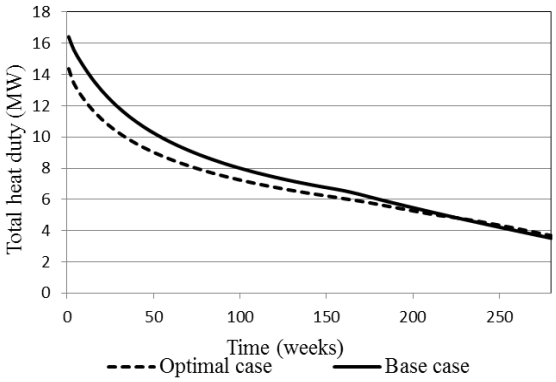

Fig. 5 Total heat load in the heat exchanger network.

The fouling rate in each heat exchanger in the base case is shown in Fig. 6.

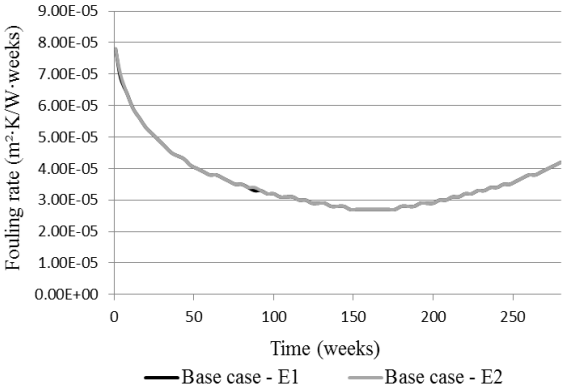

Fig. 6 Fouling rates in the base case.

In the first part of the time horizon, the accumulation of the deposits decreases the surface temperature, which brings a reduction of the fouling rate in both heat exchangers. However, in the second part, the total flow rate reduction brings a strong decrease in the flow velocity, which causes an increase of the fouling rate. There is a difference between the fouling rates, but in this example, it is small.

The fouling rate in each heat exchanger from the optimization results is shown in Fig. 7.

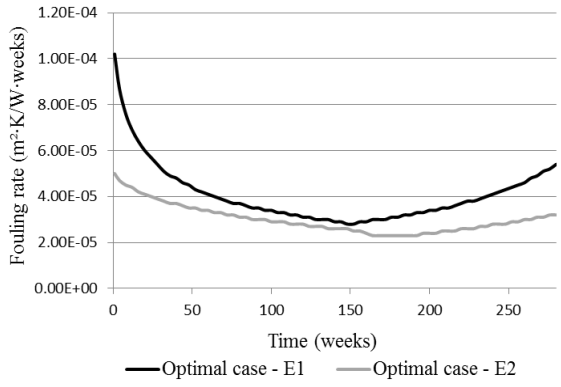

Fig. 7 Fouling rates in the optimal case.

According to this figure, the fouling rate is larger in the initially dirty heat exchanger. This pattern occurs because this unit receives a larger portion of the hot stream flow rate, which determines a higher surface tube temperature, therefore favoring fouling. This difference is intensified in the second part of the time horizon when there is a considerable flow rate deviation of the cold stream to the initially clean heat exchanger, which reduces the fouling rate increase in this unit. The trend of both fouling rates, associating a decreasing period and an increasing period, is similar to the base case.

The profiles of the thickness of the fouling layer in the base case for each heat exchanger during the operation is displayed in Fig. 8. Both curves are characterized by the growth of the thickness due to the deposit accumulation (the set of "platforms" in this figure is consequence of the numerical approximation).

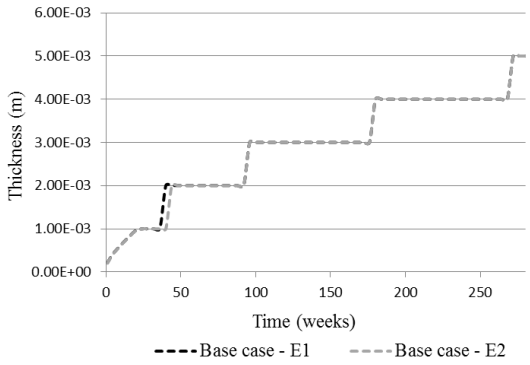

Fig. 8 Fouling layer thickness in the base case.

The profiles of the fouling layers in each heat exchanger in the optimal case is present in Fig. 9. Because of heat exchanger E1 presents a higher fouling rate (see Fig. 7), its fouling layer is thicker.

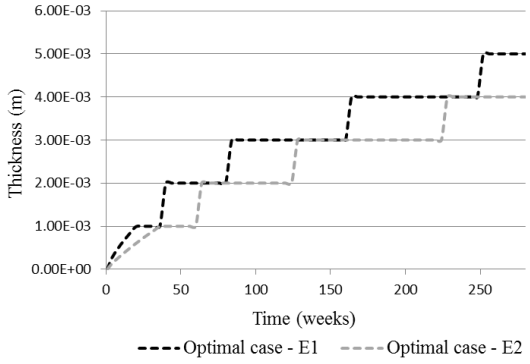

Fig. 9 Fouling layer thickness in the optimal case.

The profiles of the pressure drop in the heat exchangers in the base case are depicted in Fig. 10, because of the continuous deposit accumulation, the pressure drops always increase during the time horizon, but the increase rate is reduced after the total flow rate decreases. The difference between each heat exchanger is also small.

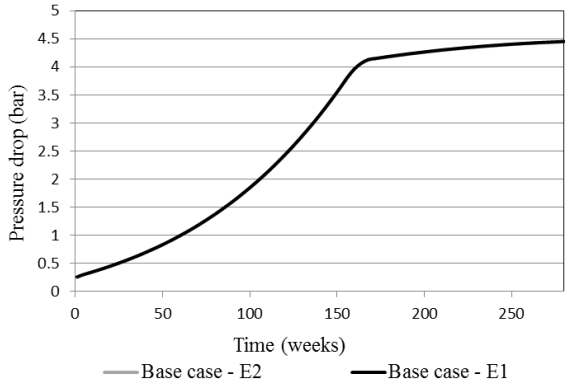

Fig. 10 Heat exchangers pressure drop in the base case.

The pressure drop profiles for the optimization results are shown in Fig. 11. In this case, the same general pattern of the pressure drop increase also occurs, but it is interesting to observe that, at the final portion of the time horizon, the pressure drop in each heat exchanger is the same, because both valves are fully open to allow the largest throughput.

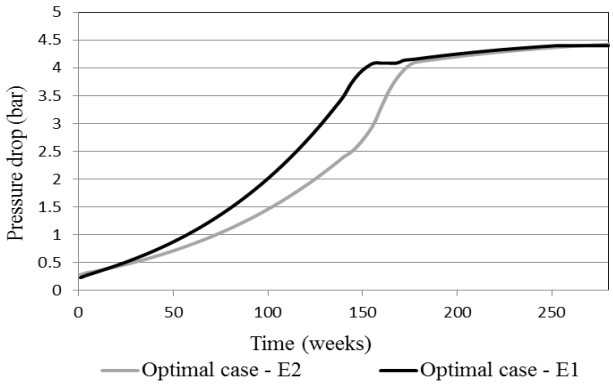

Fig. 11 Heat exchangers pressure drop in the optimal case.

CONCLUSIONS

This paper presented a procedure for the optimization of the flow rate distribution along heat exchanger networks for fouling mitigation. The proposed optimization scheme is able to identify the best flow rate profile for each parallel branch, thus reducing the total cost, which encompasses energy and production losses costs.

The numerical results indicated that this approach can obtain better results when compared with an equal distribution of the flow rate in identical parallel units.

NOMENCLATURE

A	heat exchanger area (m^2)
Cop	utility costs ($/J)
Cp	stream heat capacity (J/(kgK))
CP	network inlet/outlet stream heat capacity (J/(kgK))
CR	ratio between heat capacity flow rates
CSTR	subset of cold streams
d	pipe diameter (m)
D	tube diameter (m)
dRfdt	fouling rate (m^2K/J)
f	Fanning friction factor (dimensionless)
fobj	objective function ($)

k	subsets of streams
k_f	thermal conductivity of the deposit (W/mK)
k_w	thermal conductivity of the tube wall (W/mK)
HE	subset of heat exchangers
$HSTR$	subset of hot streams
m	stream mass flow rate (kg/s)
MX	subset of mixers
n	network inlet/outlet mass flow rate (kg/s)
Npt	number of tube passes
Ntt	total number of tubes
NTU	number of transfer units (dimensionless)
p	weights of the numerical integration procedure
P	effectiveness (dimensionless)
PD	subset of demand units
PS	subset of supply units
PU	subset of pumps
Pr	Prandtl number
Q	heat load (W)
Re	Reynolds number (dimensionless)
R_f	fouling resistance (m^2K/W)
R_{gas}	universal gas constant (J/kmolK)
R_k	valve coeficient
s	present worth factor
S	subset of streams
SCC	subset of countercurrent heat exchangers
SEC	set of sections
SMP	subset of multipass heat exchangers
SP	subset of splitters
STR	set of edges
t	subset of vertices
T	stream temperature (ºC)
TI	set of time instants
U	overall heat transfer coefficient ($W/(m^2K)$)
v	fluid velocity (m/s)
V	network inlet/outlet temperature (ºC)
VET	set of vertices

Greek symbols

ΔP_{HE}	pressure drop in a heat exchanger (Pa)
ΔP_{pipe}	pressure drop in a pipe (Pa)
ΔP_{pump}	pressure variation at the pump (Pa)
ΔP_{valve}	pressure drop in a valve (Pa)
ΔP_{SEC}	pressure drop in a section (Pa)
ΔP_{BR}	pressure drop in a branch (Pa)
ρ	density (kg/m^3)
μ	viscosity (Pa·s)

Subscript

c	cold stream
h	hot stream
i	inlet
o	outlet
in	edges into a vertex
out	edges from a vertex
f	fouled
ref	temperature reference
r	index of the branches
s	index of the sections
k	index of the edges (process streams)
$k´$	alias of index k
$k´´$	alias of index k
t	index of the vertices (network elements)
τ	index of time instants
$tube$	tube-side
$shell$	shell-side
1	heat exchnager end
2	heat exchanger end

Superscripts

$base$	base
spe	specification
spt	set-point
c	clean
d	dirty

REFERENCES

Assis, B. C. G., Gonçalves, C. O., Liporace, F. S., Oliveira, S. G., Queiroz, E. M., Pessoa, F. L. P., Costa, A. L. H., 2013, Constrained thermohydraulic optimization of the flow rate distribution in crude preheat trains, *Chem. Eng. Res. Des.*, Vol. 91, pp. 1517-1526.

Assis, B. C. G., Lemos, J. C., Liporace, F. S., Oliveira, S. G., Queiroz, E. M., Pessoa, F. L. P., Costa, A. L. H., 2015, Dynamic optimization of the flow rate distribution in heat exchangers networks for fouling mitigation, *Ind. Eng. Chem. Res.*, submitted for publication.

Ishiyama, E. M., Paterson, W. R., Wilson, D. I., 2008, Thermo-hydraulic channelling in parallel heat exchangers subject to fouling, *Chem. Eng. Sci.*, Vol. 63, pp. 3400-3410.

Oliveira Filho, L. O., Liporace, F. S., Queiroz, E. M., Costa, A. L. H., 2009, Investigation of an alternative operating procedure for fouling management in refinery crude preheat trains, *Appl. Therm. Eng.*, Vol. 29, pp. 3073-3080.

Shah, R. K., Sekulic, D. P., 2003, *Fundamentals of heat exchanger design*, John Wiley and Sons, Hoboken, New Jersey.

Yeap, B. L., Wilson, D. I., Polley, G. T., Pugh, S. J., 2005, Retrofitting crude oil refinery heat exchanger networks to minimize fouling while maximizing heat recovery, *Heat Transfer Eng.*, Vol. 26, pp. 23-34